Different particle alignments in $N \approx Z$ Ru isotopes studied by the shell model

M. Hasegawa,[1] K. Kaneko,[2] T. Mizusaki,[3,4] and S. Tazaki[5]
[1]*Laboratory of Physics, Fukuoka Dental College, Fukuoka 814-0193, Japan*
[2]*Department of Physics, Kyushu Sangyo University, Fukuoka 813-8503, Japan*
[3]*Institute of Natural Sciences, Senshu University, Kawasaki, Kanagawa 214-8580, Japan*
[4]*Institute for Solid State Physics, University of Tokyo, Kashiwanoha, Kashiwa 277-8581, Japan*
[5]*Department of Applied Physics, Fukuoka University, Fukuoka 814-0180, Japan*
(Received 9 May 2003; published 18 March 2004)

Experimentally observed heaviest $N \approx Z$ nuclei, Ru isotopes, are investigated by the shell model on a spherical basis with the extended $P+QQ$ Hamiltonian. The energy levels of all the Ru isotopes can be explained by the shell model with a single set of force parameters. The calculations indicate an enhancement of quadrupole correlations in the $N=Z$ nucleus ^{88}Ru as compared with the other Ru isotopes, but the observed moments of inertia seem to require much more enhancement of quadrupole correlations in ^{88}Ru. It is discussed that the particle alignment takes place at 8^+ in ^{90}Ru but is delayed in ^{88}Ru till 16^+ where the simultaneous alignments of proton and neutron pairs take place. The calculations present interesting predictions for ^{89}Ru that the ground state is the $1/2^-$ state and there are three $\Delta J=2$ bands with different particle alignments including the $T=0$ p-n pair alignment.

DOI: 10.1103/PhysRevC.69.034324 PACS number(s): 21.10.Hw, 21.10.Re, 21.60.Cs, 23.20.Lv

I. INTRODUCTION

The so-called delay of alignment in the $N=Z$ even-even nuclei is observed in the $64 \leqslant A \leqslant 88$ region [1–4] and in the lighter nucleus ^{48}Cr. This phenomenon is a sign of strong proton-neutron (p-n) correlations in the same shell [5], and the special collectivity in the $N=Z$ even-even nuclei suggests a strong collaboration of p-p, n-n, and p-n correlations in the $A=4m$ nuclei with $N=Z=2m$ which can be called the α-like ($T=0$) $2p$-$2n$ correlations [6–8]. A theoretical investigation of this is challenging, which belongs to the study of the properties of the p-n interaction in $N=Z$ nuclei [9–15]. The experimental study of heavy $N=Z$ nuclei has reached ^{88}Ru [3,4]. The new data have revealed that there is a remarkable difference between neighboring even-even nuclei with $N=Z$ and $N=Z+2$ in the $1g_{9/2}$-subshell region. The qualitative difference between ^{88}Ru and ^{90}Ru (^{84}Mo and ^{86}Mo) in the backbending plots of the yrast bands is different from the conditions in lighter nuclei Zr, Sr, etc., and casts a new light on the problem of the delayed alignment.

A theoretical explanation of the delayed alignment for heavy $N=Z$ nuclei ^{84}Mo, ^{88}Ru, etc., is presented in Refs. [4,16] with the projected shell model on the deformed basis [17,18]. The projected shell model reproduces the graphs of observed moments of inertia, by adopting commonly accepted deformations for those nuclei. The adopted deformations manifest that the deformation is larger for even-even $N=Z$ nuclei when compared with $N>Z$ nuclei. In other words, the delayed alignment in ^{88}Ru is related to the large deformation. The study with the projected shell model [4,15] suggested an enhancement of the p-n quadrupole-quadrupole (QQ) interaction in the $N=Z$ nuclei. It is our interest to understand the structural difference between the $N=Z$ even-even nucleus ^{88}Ru and neighboring isotopes in various aspects. In this paper, we make the study using the shell model calculations on the spherical basis which is free from fixing the deformation parameter.

The extended $P+QQ$ model [19,20] reproduces observed energy levels and $B(E2)$ in $N \approx Z$ $1f_{7/2}$-subshell nuclei and is capable of describing the backbending phenomena. It has successfully clarified characteristics of the structure of a heavier $N=Z$ nucleus ^{64}Ge in the configuration space $(2p_{3/2},1f_{5/2},2p_{1/2},1g_{9/2})^8$ in a recent shell model calculation [21]. The heaviest $N=Z$ nucleus experimentally observed, ^{88}Ru, which is expected to have the approximate configuration $(2p_{3/2},1f_{5/2},2p_{1/2},1g_{9/2})^{-12}$, is a good target to study the delayed alignment using the shell model calculation. The success in ^{64}Ge suggests that the extended $P+QQ$ model provides a reliable interaction for the study of the heavy $N \approx Z$ nuclei. We carry out shell model calculations using the extended $P+QQ$ model with a single set of force parameters fixed for ^{88}Ru and heavier Ru isotopes. The calculations, which are carried out with the calculation code [22], have huge dimensions (maximum dimension is 165×10^6 for ^{88}Ru) and can be regarded as realistic ones. We investigate the structure of Ru isotopes and examine whether the difference between ^{88}Ru and ^{90}Ru is reproduced or not by the spherical shell model, in Sec. III. The present shell model predicts interesting features of the odd-A isotope ^{89}Ru between ^{88}Ru and ^{90}Ru. The prediction for ^{89}Ru is shown in Sec. IV.

Since the delayed alignment in ^{88}Ru seems to be related to the strong quadrupole correlations and the large quadrupole deformation [4,15], we pay attention to the role of the QQ force which induces the quadrupole correlations and deformation. It is interesting to see the competition between the like-nucleon (p-p and n-n) interaction and p-n interaction of the QQ force. We also examine a possible contribution of the isovector QQ force to the properties of Ru isotopes.

II. THE MODEL HAMILTONIAN

The extended $P+QQ$ Hamiltonian is given by

$$\begin{aligned} H &= H_{\mathrm{sp}} + H_{\mathrm{mc}} + H_{P_0} + H_{P_2} + H_{QQ}^{\tau=0} + H_{OO}^{\tau=0} \\ &= \sum_{\alpha} \varepsilon_a c_\alpha^\dagger c_\alpha + H_{\mathrm{mc}} - \sum_{J=0,2} \frac{1}{2} g_J \sum_{M\kappa} P_{JM1\kappa}^\dagger P_{JM1\kappa} \\ &\quad - \frac{1}{2}\frac{\chi_2^0}{b^4}\sum_M :Q_{2M}^\dagger Q_{2M}: - \frac{1}{2}\frac{\chi_3^0}{b^6}\sum_M :O_{3M}^\dagger O_{3M}:, \end{aligned} \tag{1}$$

where ε_a is a single-particle energy, H_{mc} denotes the monopole corrections, $P_{JMT\kappa}$ is the pair operator with angular momentum J and isospin T, and Q_{2M} (O_{3M}) is the isoscalar quadrupole (octupole) operator (see Ref. [20]). The force strengths χ_2^0 and χ_3^0 are defined so as to have the dimension of energy. Following Ref. [21], we adopt the model space $(2p_{3/2}, 1f_{5/2}, 2p_{1/2}, 1g_{9/2})$ and introduce the isoscalar octupole-octupole force $H_{OO}^{\tau=0}$. Note that the Hamiltonian is isospin invariant and includes the p-n pairing forces in addition to the p-n QQ force.

The isoscalar QQ force $H_{QQ}^{\tau=0}$ can be divided into three parts, p-p, n-n, and p-n. We shall use the notations χ_{2pp}^0, χ_{2nn}^0, and χ_{2pn}^0 for their force strengths. In terms of the pair operators $P_{JMT\kappa}$, the isoscalar QQ force is expressed as

$$\begin{aligned} H_{QQ}^{\tau=0} &= -\frac{1}{2}\sum_\kappa \frac{x_\kappa^1}{b^4}\sum_{JM} W_{JT=1} P_{JM1\kappa}^\dagger P_{JM1\kappa} \\ &\quad - \frac{1}{2}\frac{x_{\kappa=0}^0}{b^4}\sum_{JM} W_{JT=0} P_{JM00}^\dagger P_{JM00}, \end{aligned} \tag{2}$$

where $x_\kappa^1 = x_{\kappa=0}^0 = \chi_2^0$. The symbol W_{JT} proportional to the Racah coefficient really has four subscripts related to the four orbits of $c_\alpha^\dagger c_\beta^\dagger c_\delta c_\gamma$. The first line of Eq. (2) brings about the isovector pairing interactions, where the strengths $x_{\kappa=1}^1$, $x_{\kappa=-1}^1$, and $x_{\kappa=0}^1$ stand for the n-n, p-p, and p-n interactions. The second line of Eq. (2) brings about the isoscalar p-n pairing interactions. The p-n part of $H_{QQ}^{\tau=0}$ is enhanced by enlarging the force strength χ_{2pn}^0 ($x_{\kappa=0}^1$ and $x_{\kappa=0}^0$) in Refs. [4,15,21]. The Hamiltonian ceases to be isospin invariant, with the isospin not being a good quantum number there.

There is a possibility of the isovector QQ force contributing to the collective motion in the heavy $N \approx Z$ nuclei. The isovector QQ force $H_{QQ}^{\tau=1}$ with the force strength χ_2^1 is also rewritten in the same form as Eq. (2) with the relations $x_\kappa^1 = \chi_2^1$ and $x_{\kappa=0}^0 = -3\chi_2^1$. We can write the sum of $H_{QQ}^{\tau=0}$ and $H_{QQ}^{\tau=1}$ in the same form as Eq. (2), where $x_\kappa^1 = \chi_2^0 + \chi_2^1$ and $x_{\kappa=0}^0 = \chi_2^0 - 3\chi_2^1$. If we consider a restricted sum of $H_{QQ}^{\tau=0}$ and $H_{QQ}^{\tau=1}$ with the following combination of the interaction strengths:

$$\chi_2^0 = (1+\alpha)x, \quad \chi_2^1 = -\alpha x, \tag{3}$$

the QQ force is written as

$$\begin{aligned} H_{QQ}^{\tau=0} + H_{QQ}^{\tau=1} &= -\frac{1}{2}\frac{x}{b^4}\sum_\kappa \sum_{JM} W_{JT=1} P_{JM1\kappa}^\dagger P_{JM1\kappa} \\ &\quad - \frac{1}{2}\frac{(1+4\alpha)x}{b^4}\sum_{JM} W_{JT=0} P_{JM00}^\dagger P_{JM00}. \end{aligned} \tag{4}$$

By changing the mixing parameter α, we can enhance the p-n part of the QQ force, which corresponds to the isoscalar p-n pairing interactions in the second line of Eq. (4), without violating the isospin invariance of the Hamiltonian.

III. DIFFERENCE BETWEEN ^{88}Ru AND ^{90}Ru

Using the extended $P+QQ$ Hamiltonian (1), we carried out shell model calculations in the hole space $(1g_{9/2}^h, 2p_{1/2}^h, 1f_{5/2}^h, 2p_{3/2}^h)$ with the calculation code [22]. The single-hole energies ε_a^h depend on H_{mc} and the force strengths as well as ε_a through the hole transformation. We treated the hole energies ε_a^h as parameters instead of the single-particle energies ε_a. We tried various combinations of the parameters ε_a^h, H_{mc}, g_0, g_2, χ_2^0, and χ_3^0, and determined these parameters so as to reproduce overall energy levels of the Ru isotopes. The adopted parameters are

$$\begin{gathered} \varepsilon_{9/2}^h = 0.0, \quad \varepsilon_{1/2}^h = 1.1, \quad \varepsilon_{5/2}^h = 5.5, \quad \varepsilon_{3/2}^h = 6.0, \\ g_0 = 0.26(92/A), \quad g_2 = 0.12(92/A)^{5/3}, \\ \chi_2^0 = 0.26(92/A)^{5/3}, \quad \chi_3^0 = 0.04(92/A)^2 \quad \text{in} \quad \text{MeV}, \end{gathered} \tag{5}$$

and H_{mc} is fixed at zero (the J-independent isoscalar monopole term is not determined, because we do not deal with the binding energy in this paper). Changing the monopole corrections H_{mc} does not significantly improve the energy levels. The relative position of $\varepsilon_{9/2}^h$ and $\varepsilon_{1/2}^h$ is responsible for that of the positive and negative parity states. In our trials, the values of $\varepsilon_{5/2}^h$ and $\varepsilon_{3/2}^h$ listed in Eq. (5) are best and the exchange of the two values does not improve the energy levels. The hole levels $1f_{5/2}^h$ and $2p_{3/2}^h$ seem to lie far from $2p_{1/2}^h$. This is the reason why the subspace $(2p_{1/2}, 1g_{9/2})$ works well for $A > 86$ nuclei in Refs. [23,24]. The force strengths g_0, g_2, χ_2^0, and χ_3^0 adopted are similar to those used in the study of ^{64}Ge [21].

The parameter set (5) reproduces well the energy levels (the patterns and order of the positive- and negative-parity levels) of Ru isotopes, not only the even-A nuclei ^{92}Ru and ^{94}Ru but also the odd-A nuclei ^{91}Ru and ^{93}Ru as shown in Figs. 1 and 2. The agreement between theory and experiment for the odd-parity state is worse than that for the even-parity states. The calculation, however, reproduces the observed energies within the error 0.8 MeV.

A. Dependence on the QQ force strengths

The energy levels obtained for ^{88}Ru and ^{90}Ru, which are shown in the column A of Figs. 3 and 4, are consistent with the observed ones. The parameter set A describes the difference between ^{88}Ru and ^{90}Ru in the backbending plot (we call it "J-ω graph") as shown in Figs. 5 and 6. The calculation

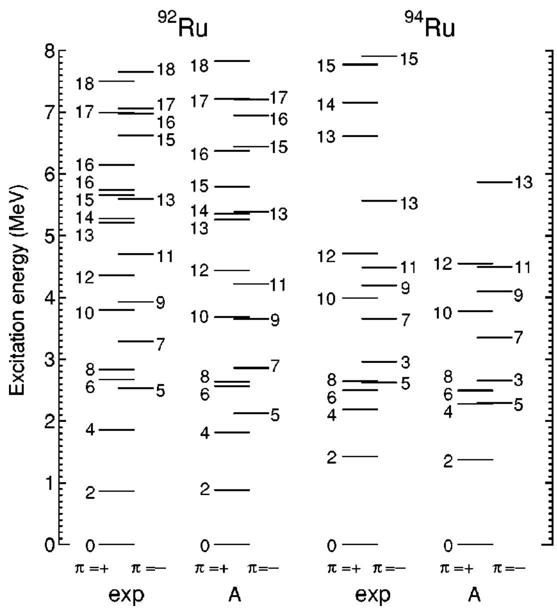

FIG. 1. Energy levels of ^{92}Ru and ^{94}Ru. The label "*A*" stands for the energy levels calculated with the parameter set (5) and "exp" for the observed ones.

reproduces the sharp backbending at $J=2j-1=8$ observed in ^{90}Ru and shows no clear backbending in low-spin states of ^{88}Ru in agreement with the experiment.

The backbending plots, however, reveal insufficiency for the most collective low-lying states. The results *A* do not reproduce the slope of the J-ω graph up to $J=8$ for ^{88}Ru and up to $J=6$ for ^{90}Ru. The slopes of the J-ω graphs for the collective bands are considerably affected by the strength χ_2^0 of the QQ force $H_{QQ}^{\tau=0}$ above all other force strengths. This is naturally understood, because the moment of inertia of a rotational band depends on the magnitude of deformation and

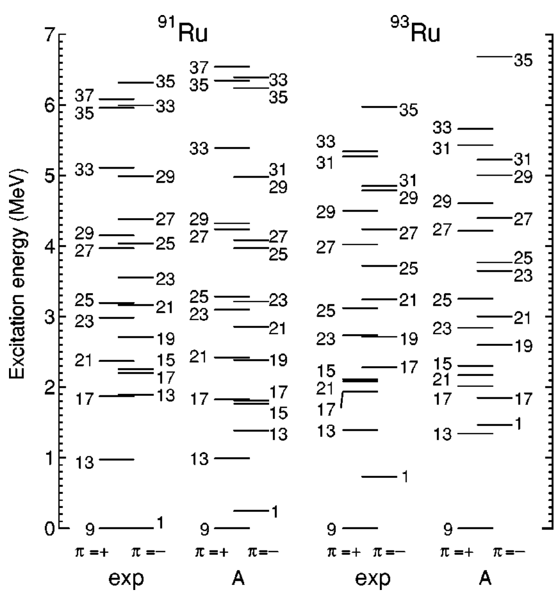

FIG. 2. Calculated and observed energy levels of ^{91}Ru and ^{93}Ru. The spin of each state is denoted by the double number $2J$.

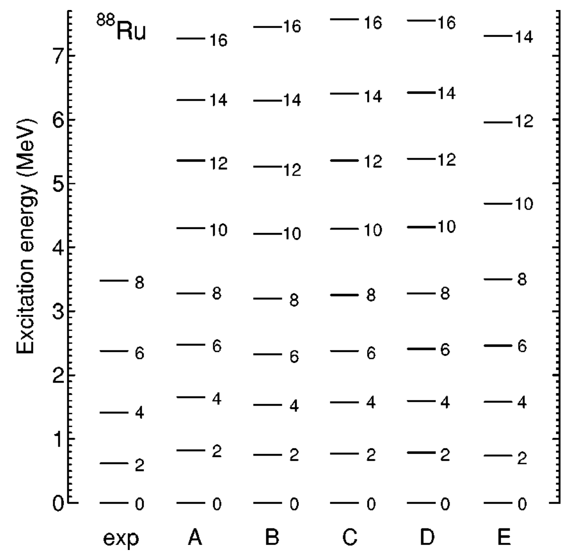

FIG. 3. Comparison of calculated energy levels with observed ones for ^{88}Ru. The calculated results are obtained with the different strengths of the QQ force, *A*, *B*, *C*, *D*, and *E*.

the QQ force drives the quadrupole deformation. Let us try to improve the J-ω graphs for ^{88}Ru and ^{90}Ru by readjusting the QQ force strength.

We first strengthen the p-n QQ interaction by adding the isovector QQ force $H_{QQ}^{\tau=1}$ in the form (4) so as to conserve the isospin invariance. The results obtained with the mixing parameter $\alpha=0.125$ [see Eq. (3)] are shown by the notation *B* in Figs. 3–6. The J-ω graph is improved for ^{90}Ru. For ^{88}Ru, the result *B* removes the slight backbending at $J=8$ of the result *A*. The parameter set *B* reproduces quite well the overall energy levels of the Ru isotopes ^{90}Ru, ^{91}Ru, ^{92}Ru, ^{93}Ru, and ^{94}Ru. For the high-spin states, however, the parameter set *A* is better than *B*. The change from *A* to *B* pushes up the high-spin levels higher as the spin *J* increases. Since the

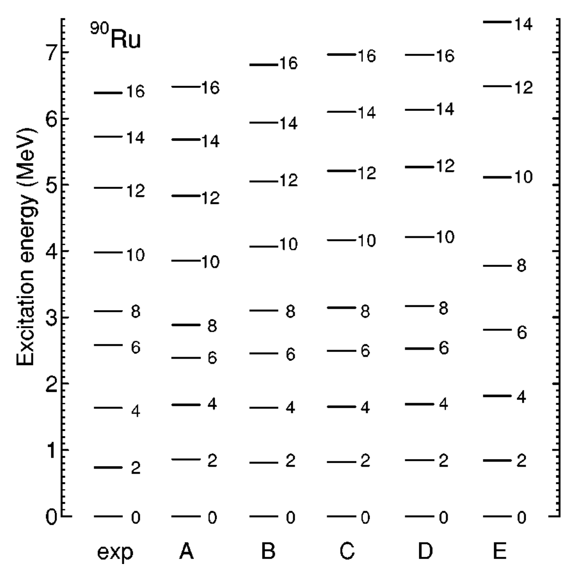

FIG. 4. Comparison of calculated energy levels with observed ones for ^{90}Ru. The calculated results are obtained with the different strengths of the QQ force, *A*, *B*, *C*, *D*, and *E*.

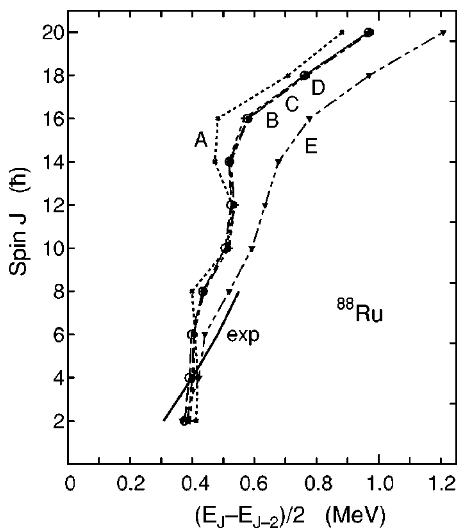

FIG. 5. The *J*-ω graph of Fig. 1.

configuration $(1g^h_{9/2})^m$ is dominant in the high-spin states, the inadequacy for the high-spin states suggests that the enhanced *p-n QQ* force strength ($x^0_{\kappa=0}=1.5x$) is too strong for the $1g_{9/2}$ subshell. The remaining deviation of the calculated *J*-ω graph from the experimental one for ^{88}Ru indicates room for improvement in the model space and in the interactions of our model.

Results similar to those of *B* are obtained by strengthening the *p-n* part of the isoscalar *QQ* force $H^{\tau=0}_{QQ}$ (by enlarging χ^0_{2pn}). The results of $\chi^0_{2pn}=1.25\chi^0_{2pp}$ are shown by the notation *C* in Figs. 3–6. (Note that the *p-n* force strength $\chi^0_{2pn}=1.3\chi^0_{2pp}$ is used by Sun *et al.* [4] to increase the particle alignment frequency for ^{88}Ru and ^{84}Mo.) Although the high-spin levels of *C* are pushed up a little higher as compared with those of *B*, the parameter sets *B* and *C* yield similar results, not only for the energy levels but also for $B(E2)$ values and the quadrupole moment *Q* with respect to the yrast bands of ^{88}Ru and ^{90}Ru as shown later on. We also tried to strengthen all of the *p-p*, *n-n*, and *p-n QQ* interactions. The enlargement of χ^0_2 to $1.1\times\chi^0_2$ yields results similar to those of *B* and *C*. The results are denoted by *D* in Figs. 3–6. Within the small increase of the *QQ* force, we have found no evidence that the *p-n QQ* interaction is stronger than the *p-p* and *n-n QQ* interactions, and there is no choice between the isospin-variant and isospin-invariant enhancements of the *p-n QQ* interaction, as well.

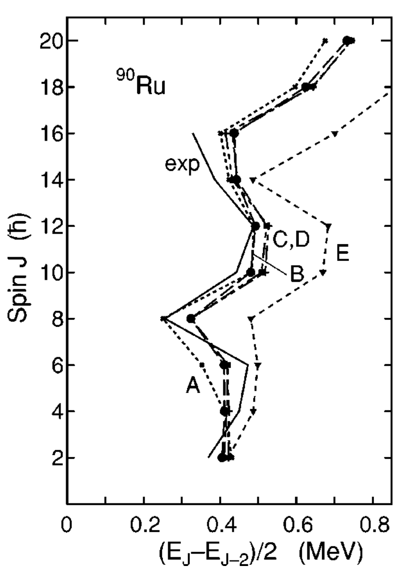

FIG. 6. The *J*-ω graph of Fig. 2.

It should be noted here that the strength of the *p-n* interaction does not directly correspond to the strength of the *p-n* correlations. According to the single-*j* shell calculation with the extended $P+QQ$ force [25], the *p-n* correlation energy becomes largest at $N=Z$ in nuclei with the same *Z* even though the same *p-n* interaction is used for those nuclei, while the *p-p* and *n-n* correlation energy does not show such a specific feature.

In Fig. 5, the discrepancy between the calculated moments of inertia (*B*, *C*, and *D*) and observed ones is still large for ^{88}Ru. The calculations *B*, *C*, and *D* cannot sufficiently reproduce the observed large angular frequency at $J=8$. If we want to obtain a better slope of the *J*-ω graph for ^{88}Ru, we must enhance the *QQ* force strength χ^0_2 much more. The slope of the *J*-ω graph observed in ^{88}Ru cannot be well reproduced even by strengthening the *p-n QQ* interaction further in the way *B* or *C*. Results obtained with the isoscalar *QQ* force $H^{\tau=0}_{QQ}$ strengthened by 1.5 $(1.5\times\chi^0_2)$ are denoted by *E* in Figs. 3–6. The calculation *E* reproduces the large angular frequency and the slope (moment of inertia) of the *J*-ω graph for ^{88}Ru but yields rather bad results for ^{90}Ru. This suggests that the collectivity of the quadrupole correlations is different between ^{88}Ru and ^{90}Ru. The observed moment of inertia and large angular frequency indicate a stable rotation of ^{88}Ru, while the energy levels and the sharp backbending at 8^+ reveal a deviation from the rotation in ^{90}Ru. Our spherical shell model calculation predicts that clear backbending does not occur up to $J=14$ in ^{88}Ru, as predicted by the projected shell model [4,16]. The present results indicate a special enhancement of the quadrupole correlations in ^{88}Ru in contrast to the other Ru isotopes with $N>Z$. This is consistent with the results obtained by the projected shell model [4,16], in which the deformation parameter is fixed to be 0.23 for ^{88}Ru and 0.16 for ^{90}Ru (the former is 1.4 times as large as the latter). Our spherical shell model requires the enhancement of the *QQ* force instead of the enlargement of the deformation for the $N=Z$ nucleus ^{88}Ru. This suggests that the present model space $(2p_{3/2},1f_{5/2},2p_{1/2},1g_{9/2})$ may not be sufficient and the lower orbit $1f_{7/2}$ or the upper one $2d_{5/2}$ should be included possibly.

B. Difference between ^{88}Ru and ^{90}Ru in structure

The backbending at $J=2j-1=8$ in the $1g_{9/2}$-subshell nucleus ^{90}Ru is in contrast to no backbending at $J=2j-1=6$ in the $1f_{7/2}$-subshell nucleus ^{50}Cr, while the resistance to the backbending is common to the $N=Z$ nuclei ^{88}Ru and ^{48}Cr. Let us discuss the difference between ^{88}Ru and ^{90}Ru in the structure which appears in the *J*-ω graphs of Figs. 5 and 6. In Tables I and II, we tabulate the expectation values of proton and neutron numbers $\langle n_a\rangle$ in the respective orbits for

TABLE I. Expectation values of proton (neutron) numbers in the respective orbits for the yrast states of ^{88}Ru calculated with the different strengths of the QQ force, A and B.

J	$p_{3/2}$	$f_{5/2}$	$p_{1/2}$	$g_{9/2}$
		Cal. A		
0	3.87	5.74	0.73	5.66
2	3.85	5.72	0.68	5.75
4	3.84	5.71	0.62	5.84
6	3.82	5.68	0.59	5.90
8	3.83	5.69	0.66	5.86
10	3.82	5.67	0.61	5.89
12	3.81	5.66	0.57	5.96
14	3.82	5.67	0.57	5.94
16	3.85	5.72	0.71	5.71
18	3.86	5.73	0.78	5.63
20	3.98	5.97	0.91	4.13
		Cal. B		
0	3.80	5.65	0.65	5.89
2	3.79	5.63	0.66	5.92
4	3.78	5.62	0.65	5.95
6	3.77	5.60	0.66	5.96
8	3.77	5.60	0.66	5.96
10	3.77	5.59	0.67	5.98
12	3.76	5.58	0.66	5.99
14	3.77	5.59	0.65	5.99
16	3.78	5.60	0.65	5.97
18	3.78	5.60	0.65	5.97
20	3.78	5.59	0.65	5.98

TABLE II. Expectation values of proton and neutron numbers in the respective orbits for the yrast states of ^{90}Ru calculated with the different strengths of the QQ force, A and B.

	Proton				Neutron			
J	$p_{3/2}$	$f_{5/2}$	$p_{1/2}$	$g_{9/2}$	$p_{3/2}$	$f_{5/2}$	$p_{1/2}$	$g_{9/2}$
				Cal. A				
0	3.94	5.87	1.08	5.11	3.99	5.96	1.84	6.21
2	3.93	5.86	1.00	5.20	3.99	5.97	1.88	6.16
4	3.93	5.87	1.01	5.19	3.99	5.98	1.94	6.09
6	3.96	5.90	1.41	4.73	3.99	5.98	1.94	6.08
8	3.97	5.93	1.64	4.46	3.99	5.97	1.88	6.16
10	3.98	5.95	1.77	4.30	3.99	5.98	1.92	6.12
12	3.98	5.97	1.89	4.16	3.99	5.98	1.95	6.07
14	3.98	5.96	1.81	4.25	3.99	5.99	1.96	6.06
16	3.97	5.95	1.64	4.44	3.99	5.99	1.97	6.05
18	3.98	5.96	1.74	4.32	3.99	5.99	1.98	6.03
20	3.99	5.98	1.88	4.15	3.99	5.99	1.98	6.03
				Cal. B				
0	3.91	5.83	0.86	5.39	3.98	5.94	1.79	6.29
2	3.90	5.82	0.78	5.49	3.98	5.95	1.84	6.23
4	3.90	5.82	0.76	5.52	3.98	5.97	1.91	6.14
6	3.93	5.86	1.12	5.09	3.99	5.98	1.95	6.08
8	3.97	5.92	1.60	4.51	3.98	5.97	1.88	6.17
10	3.98	5.95	1.78	4.30	3.99	5.97	1.91	6.13
12	3.98	5.97	1.88	4.17	3.99	5.98	1.96	6.07
14	3.97	5.95	1.73	4.34	3.99	5.99	1.97	6.05
16	3.96	5.93	1.55	4.56	3.99	5.99	1.97	6.05
18	3.97	5.94	1.68	4.40	3.99	5.99	1.98	6.03
20	3.99	5.97	1.88	4.16	3.99	5.99	1.98	6.03

the yrast states of ^{88}Ru and ^{90}Ru. The tables show that more protons jump up from the pf subshell to the $1g_{9/2}$ one in ^{88}Ru than in ^{90}Ru, and the same is true for neutrons if the extra neutron pair is subtracted from the neutron number $\langle n_{g9/2}\rangle$ for ^{90}Ru. Two things are characteristic in the $N \approx Z$ Ru isotopes, which is different from the situation of the $N \approx Z$ Cr isotopes in the $1f_{7/2}$ subshell. First, the $1g_{9/2}$ subshell where the Fermi level lies is just above the pf subshell and there is a considerably large degree of freedom for $1g_{9/2}$. Second, the two subshells have opposite parities. These conditions permit only nucleon pairs jumping up to $1g_{9/2}$ and induce strong p-p, n-n, and p-n correlations in $1g_{9/2}$. We can suppose that the collaboration of the p-p, n-n, and p-n correlations results in the α-like $2p$-$2n$ correlations especially in the $1g_{9/2}$ subshell, in the $N=Z$ nucleus ^{88}Ru where the p-n correlations are enhanced.

The sharp backbending at 8^+ in Fig. 6 for ^{90}Ru coincides with the increase of $\langle n_{g9/2}\rangle$ and decrease of $\langle n_{p1/2}\rangle$ for neutron (and their decrease and increase for proton) at $J=8$ in Table II. This change is explained by the alignment of a neutron pair in $1g_{9/2}$. The results A and B in Table II suggest the following explanation. There is an extra neutron pair which cannot form a $T=0$ $2p$-$2n$ quartet [7,8,26] in ^{90}Ru. The extra neutron pair has a dominant probability to be a pair with $J=0$ and $T=1$, and contributes to the collective $2p$-$2n$ correlations through the exchange with a neutron pair in the quartets. The excitation till 6^+ owes to the motion of the quartets. At 8^+, the extra neutron pair aligns the angular momentum to be $J=9/2+7/2$ $(J=8, T=1)$ in $1g_{9/2}$ and breaks away from the collective $2p$-$2n$ correlations, which increases the $1g_{9/2}$ neutron number. The weakened $2p$-$2n$ correlations somewhat hinder proton pairs jumping up to the $1g_{9/2}$ subshell from the pf subshell, which decreases the $1g_{9/2}$ proton number. The result A for ^{88}Ru in Table I shows a similar sign at $J=8$, but the observed J-ω graph denies such a pair alignment in ^{88}Ru. The calculated results B, C, D, and E which are better for the very collective low-lying states sweep away the sign of a structural change in $\langle n_a\rangle$ (the result B is shown in the lower part of Table I). By combining our result for ^{88}Ru with the J-ω graphs experimentally observed in other $N=Z$ nuclei, we can say that the one-pair alignment is hindered in the $N=Z$ nuclei due to the strong $2p$-$2n$ correlations. This may be the reason for the durable increase of angular frequency in the $N=Z$ nuclei.

Instead, Fig. 5, in which the monotonous slope after $J=16$ stands out, suggests a structure change at 16^+ in ^{88}Ru. The projected shell model [4,16] also predicts a backbending at $J=16$ for ^{88}Ru. Moreover, the calculated result A in Table I shows the increase of $\langle n_{f5/2}\rangle$ and $\langle n_{p1/2}\rangle$, and the decrease of

$\langle n_{g9/2} \rangle$ at $J=16$. The same sign remains slightly in $\langle n_{g9/2} \rangle$ of the result B and the sign disappears for the strong QQ force E. As mentioned above, however, the enhanced QQ force of B, C, D, and E is more or less too strong for the high-spin states. We can expect that the structural change at $J=16$ will be observed in ^{88}Ru. This structural change seems to be caused by the simultaneous alignments of proton and neutron pairs at $J=2\times(9/2+7/2)$, since the strong $2p$-$2n$ correlations resist the single alignment of proton or neutron pair. The analysis in Ref. [27], which predicts the simultaneous alignments of proton and neutron pairs at $J=2\times(7/2+5/2)$ without backbending due to the one-pair alignment in the $1f_{7/2}$ $N=Z$ nucleus ^{48}Cr, supports our conjecture for the $1g_{9/2}$ $N=Z$ nucleus ^{88}Ru. This conjecture is also supported by the backbending toward $J=16$ observed in ^{90}Ru. In Table II, the increase of proton number $\langle n^{\pi}_{g9/2} \rangle$ at $J=16$ in the results A and B for ^{90}Ru suggests the proton-pair alignment in $1g_{9/2}$ in addition to the neutron-pair alignment at $J=8$.

C. Effect of the $2d_{5/2}$ orbit

The large deformation on the deformed basis can be interpreted by the mixing of a large number of spherical single-particle orbits. The expansion of the configuration space instead of the enhancement of the QQ force is effective in our spherical shell model. The $2d_{5/2}$ orbit could contribute to the quadrupole correlations, because it strongly couples with the $1g_{9/2}$ orbit which plays a leading role in the Ru isotopes, through the large matrix element $\langle 1g_{9/2} \| Q \| 2d_{5/2} \rangle$. Adding the $2d_{5/2}$ orbit to the model space $(2p_{3/2}, 1f_{5/2}, 2p_{1/2}, 1g_{9/2})$, unfortunately, makes the number of the shell model basis states too huge. Instead of this, let us examine the contribution of the $2d_{5/2}$ orbit within the truncated space $(2p_{1/2}, 1g_{9/2}, 2d_{5/2})$. This space does not cause the spurious motion of the center of mass, and is expected to work well as the truncated space $(1f_{7/2}, 2p_{3/2})$ without $(2p_{1/2}, 1f_{5/2})$ can explain the main features of the $f_{7/2}$-subshell nuclei [28,29] because of the large matrix element $\langle 1f_{7/2} \| Q \| 2p_{3/2} \rangle$ (the Q matrix element becomes large when $\Delta l = \Delta j = 2$). We carried out the shell model calculations using the single-particle energies $\varepsilon_{1/2}=0.0$, $\varepsilon_{9/2}=1.0$, and $\varepsilon_{5/2}=6.0$ in MeV. The inclusion of $2d_{5/2}$ allows us to use weaker force strengths than those in Eq. (5). We replaced the A dependence $(92/A)^x$ with $(88/A)^x$ for g_0, g_2, χ_2^0, and χ_3^0 in Eq. (5). The results for ^{88}Ru and ^{90}Ru are shown by the dashed lines (X) in Fig. 7.

In Fig. 7, the calculated J-ω graph agrees well with the experimental one observed for the low-lying collective states of ^{88}Ru. The agreement is better than those of B, C, and D in Fig. 5. (It is notable that Fig. 7 also predicts the alignment at $J=16$ in ^{88}Ru.) This suggests that adding the $2d_{5/2}$ orbit to $(2p_{3/2}, 1f_{5/2}, 2p_{1/2}, 1g_{9/2})$ with adjusted force strengths probably improves the calculated results for ^{88}Ru. The collectivity in the expanded space could enhance the quadrupole correlations without strengthening the QQ force. Since the large deformation causes a large admixture of the $2d_{5/2}$ spherical orbit in the deformed Nilsson basis states, the present result is consistent with the prediction of Refs. [4,16] that the deformation of the $N=Z$ nucleus ^{88}Ru is large (0.23). In contrast to this, the inclusion of $2d_{5/2}$ ruins the J-ω graph for ^{90}Ru as shown in Fig. 7. The energy levels obtained do not display the sharp backbending at $J=8$ but look like a stable rotation. The discrepancy says that the $2d_{5/2}$ orbit must not so much join in the quadrupole correlations (or the $2d_{5/2}$ orbit must be far from $1g_{9/2}$) and hence the deformation is not large for ^{90}Ru, which is consistent with a smaller deformation (0.16) adopted in Refs. [4,16].

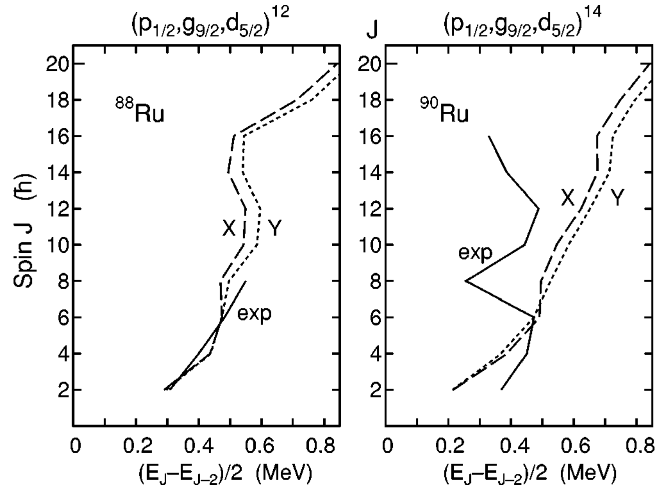

FIG. 7. The J-ω graphs obtained in the model space $(2p_{1/2}, 1g_{9/2}, 2d_{5/2})$ for ^{88}Ru and ^{90}Ru, compared with the experimental ones.

As mentioned in Ref. [19], the QQ force gives inverse magnitudes to the interaction matrix elements $\langle (g_{9/2})^2_{J,T=1} | H^{\tau=0}_{QQ} | (g_{9/2})^2_{J,T=1} \rangle$ with $J=6$ and $J=8$ contrary to those of the ordinary effective interaction [23]. This defect has a bad influence on the J-ω graph at $J=8$. If we replace the $J=6$ and $J=8$ matrix elements with those of Ref. [23], the slight backbending at $J=8$ in the calculated result for ^{88}Ru disappears as shown by the dotted line (Y) in Fig. 7. Figures 1–6 are not free from the same influence either. This defect, however, does not change the general situation.

D. $B(E2)$ and Q moment

We have discussed the energy levels, J-ω graph, and $\langle n_a \rangle$ so far. The $B(E2)$ value and Q moment are good physical quantities to see the characteristics of the quadrupole correlations. We calculated the $B(E2)$ values and Q moments for the yrast states of ^{88}Ru and ^{90}Ru, using the different strengths of the QQ force A, B, C, D, and E (corresponding to those in Figs. 3–6) and the model X (corresponding to X in Fig. 7). We used the effective charges $e_p=1.5e$ and $e_n=0.5e$, to compare the relative values of electric quadrupole quantities obtained with the different strengths of the QQ force. The calculated results are tabulated in Tables III and IV.

In Table III, the calculated $B(E2)$ values of ^{88}Ru are much larger than those of ^{90}Ru, providing that the energy levels of both nuclei are approximately reproduced. The ratios of the $B(E2)$ values are more than 1.6 in the calculation A. In other words, the quadrupole correlations are much more enhanced in the $N=Z$ nucleus ^{88}Ru than in ^{90}Ru. This is consistent with

TABLE III. $B(E2:J_i \rightarrow J_f)$ for the yrast states of ^{88}Ru and ^{90}Ru calculated with the different strengths of the QQ force, A, B, C, D, and E. The last column X shows the values obtained in the model space $(2p_{1/2}, 1g_{9/2}, 2d_{5/2})$.

	$B(E2:J_i \rightarrow J_f)$ (e^2 fm^4)					
$J_i \rightarrow J_f$	A	B	C	D	E	X
^{88}Ru						
$2 \rightarrow 0$	460	543	536	522	612	510
$4 \rightarrow 2$	630	730	722	704	832	730
$6 \rightarrow 4$	672	790	780	758	914	582
$8 \rightarrow 6$	697	847	833	806	964	601
$10 \rightarrow 8$	771	897	884	862	999	619
$12 \rightarrow 10$	775	896	882	859	999	568
$14 \rightarrow 12$	748	880	866	844	982	532
$16 \rightarrow 14$	671	853	839	814	962	489
$18 \rightarrow 16$	622	820	806	782	931	430
$20 \rightarrow 18$	71	760	748	725	872	348
^{90}Ru						
$2 \rightarrow 0$	296	339	348	339	482	567
$4 \rightarrow 2$	385	451	466	456	663	793
$6 \rightarrow 4$	294	388	418	418	698	713
$8 \rightarrow 6$	235	236	213	234	654	657
$10 \rightarrow 8$	309	322	325	331	764	673
$12 \rightarrow 10$	284	290	289	270	501	621
$14 \rightarrow 12$	257	265	227	218	600	538
$16 \rightarrow 14$	238	274	296	299	396	440
$18 \rightarrow 16$	252	275	296	300	597	413
$20 \rightarrow 18$	191	199	202	205	542	335

the fact that a larger deformation is employed for ^{88}Ru as compared with ^{90}Ru in the projected shell model [4,16].

The modifications of the QQ interaction, B, C, and D, somewhat enlarge the $B(E2)$ values both for ^{88}Ru and ^{90}Ru. The ratios of the $B(E2)$ values for ^{88}Ru to those for ^{90}Ru are still large. The very strengthened QQ force E, which is required to reproduce the slope of the J-ω graph for ^{88}Ru, enlarges the $B(E2)$ values fairly for ^{88}Ru and drastically for ^{90}Ru. We have already seen that the strengthened QQ force E ruins the pattern of energy levels for ^{90}Ru. The enhanced $B(E2)$ values in the column E of Table III are therefore too large for ^{90}Ru. We do not adopt the large $B(E2)$ values in the column X for ^{90}Ru for the same reason. The quadrupole correlations must not be enhanced too much and the contribution of the $2d_{5/2}$ orbit should be small for ^{90}Ru. Namely, ^{90}Ru may not be largely deformed. The truncated configuration space $(2p_{1/2}, 1g_{9/2}, 2d_{5/2})$ yields $B(E2)$ values comparable to those of the result A for ^{88}Ru, in spite of the small space. The expansion of the model space by adding $2d_{5/2}$ to $(2p_{3/2}, 1f_{5/2}, 2p_{1/2}, 1g_{9/2})$ can make the $B(E2)$ values larger, which could be appropriate to the enhanced quadrupole correlations in ^{88}Ru.

The calculated quadrupole moments $Q(J)$ tabulated in Table IV show the same results as the $B(E2)$ values. From Table IV, we can say as follows. The small enhancements of the p-n QQ interaction (B and C) change insignificantly the structure of ^{88}Ru and ^{90}Ru, while the strong enhancement of the QQ force by 1.5 times (E) changes the structure of ^{88}Ru drastically. The large and roughly constant Q moments of ^{88}Ru suggest the quadrupole deformation. If the result E should not be adopted for ^{90}Ru, Table IV and the energy levels insist that ^{90}Ru does not have a large deformation.

TABLE IV. Quadrupole moment $Q(J)$ in $e\,\mathrm{fm}^2$ for the yrast states of ^{88}Ru and ^{90}Ru calculated with the different strengths of the QQ force, A, B, C, D, and E.

	J	A	B	C	D	E
^{88}Ru	2	1.4	8.9	8.1	6.3	28.7
	4	−1.9	8.1	7.5	5.1	31.0
	6	20.1	28.3	27.6	25.7	41.7
	8	23.6	30.8	30.2	28.6	41.6
	10	26.6	33.3	32.7	31.3	42.1
	12	31.1	36.5	36.3	35.2	43.6
	14	32.2	37.5	37.2	36.3	43.5
	16	26.9	37.6	37.1	35.8	43.6
	18	26.6	39.5	38.9	37.6	45.2
	20	−14.9	43.1	42.5	41.5	47.8
^{90}Ru	2	−12.0	−16.4	−16.7	−15.8	−14.4
	4	−16.6	−21.6	−22.5	−21.5	−12.8
	6	12.5	5.1	4.7	3.7	15.9
	8	15.5	14.3	16.5	16.9	36.0
	10	11.5	9.9	11.7	12.2	38.8
	12	5.6	5.0	5.6	5.7	53.7
	14	−3.6	4.2	6.8	7.7	68.4
	16	1.8	4.1	7.4	8.0	36.2
	18	−0.7	0.9	3.6	4.5	33.5
	20	−4.1	−3.9	−2.7	−2.0	35.7

The calculated $B(E2)$ values and Q moments in Tables III and IV testify the structural change due to the particle pair alignment at 8^+ in ^{90}Ru, in contrast to ^{88}Ru. The $B(E2:8^+ \rightarrow 6^+)$ value decreases and Q moment increases at 8^+ in ^{90}Ru, while the two values do not show any abrupt changes at 8^+ in ^{88}Ru. On the other hand, the simultaneous alignments of proton and neutron pairs at 16^+ leave a sign in the $B(E2)$ values and Q moment in the result A both for ^{88}Ru and ^{90}Ru.

IV. PREDICTION FOR ^{89}Ru

The ^{89}Ru isotope between ^{88}Ru and ^{90}Ru has not experimentally been observed yet. Our model, however, predicts interesting features of ^{89}Ru. Figure 8 shows the energy levels and relative $B(E2)$ values obtained using the parameter set A for ^{89}Ru. The collective states connected by large $B(E2)$ values are divided into four bands. They are the yrast states except for $15/2^-$ and $31/2^+$. Exceptionally, we select the second states $(15/2)_2^-$ and $(31/2)_2^+$ as collective states based on the $B(E2)$ values and Q moments, which are adjacent to the yrast states $(15/2)_1^-$ and $(31/2)_1^+$, respectively. The relative $B(E2)$ values are denoted by the widths of the arrows in

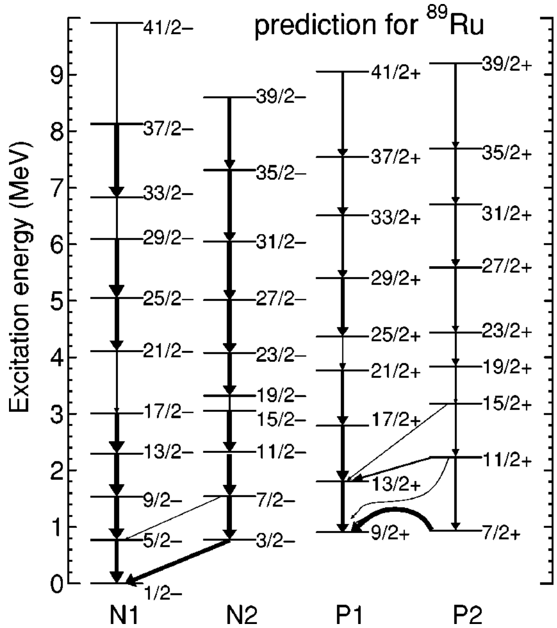

FIG. 8. Energy levels predicted for ^{89}Ru. The widths of the arrows show the relative $B(E2)$ values.

Fig. 8. The interband $E2$ transitions which are not shown in Fig. 8 are weak.

It is remarkable that the predicted ground state of the middle $1g_{9/2}$-subshell nucleus ^{89}Ru is the $1/2^-$ state. This extraordinary event is reasonable from the systematic lowering of the $1/2^-$ state with decreasing N in odd-A Ru isotopes as seen in Fig. 2. Our model reproduces the systematic behavior of $1/2^-$. Look at the expectation values of proton and neutron numbers $\langle n_a \rangle$ for the bandhead states $1/2^-$, $3/2^-$, $9/2^+$, and $7/2^+$ of ^{89}Ru which are tabulated in Table V. This table shows that the $1/2^-$ state has more protons in $1g_{9/2}$ than the $9/2^+$ state. From the comparison of Table V with Tables I and II, the $1/2^-$ state resembles the ground state of ^{88}Ru and the $9/2^+$ state resembles the ground state of ^{90}Ru. Roughly speaking, the $1/2^-$ state is constructed by adding one neutron to ^{88}Ru(0^+), and the $9/2^+$ state by removing one neutron from ^{90}Ru(0^+). The $B(E2)$ values of the negative parity bands larger than those of the positive parity bands indicate the stronger collectivity of the negative parity bands. This corresponds to the result shown in Table III that the $B(E2)$ values of ^{88}Ru are larger than those of ^{90}Ru. From these comparisons, the difference between the $1/2^-$ state and the $9/2^+$ state can be understood in terms of the α-like $2p$-$2n$ correlations mentioned in the interpretation of the difference between ^{88}Ru and ^{90}Ru. The strong α-like $2p$-$2n$ correlations pull up more protons to $1g_{9/2}$ in $1/2^-$ than in $9/2^+$, because the disturbing extra neutron is absent in $1g_{9/2}$ for the $1/2^-$ state. The inversion of $9/2^+$ and $1/2^-$ says that the α-like $2p$-$2n$ correlations give a larger energy gain to the $1/2^-$ state and the larger correlation energy compensates the energy loss of more nucleon jumps to the $1g_{9/2}$ subshell in $1/2^-$.

We can expect that the $\Delta J=2$ bands on the $1/2^-$ and $9/2^+$ states are similar to the ground-state bands of ^{88}Ru and ^{90}Ru, respectively. In fact, the J-ω graphs for the two bands $N1$ and $P1$ of ^{89}Ru which are shown in Figs. 9 and 10 are similar to those of ^{88}Ru and ^{90}Ru in Figs. 5 and 6. Figure 9 suggests no backbending at $17/2^-$ $(1/2^-+8)$ in the negative parity band $N1$, while Fig. 10 predicts a backbending phenomenon at $25/2^+$ $(9/2^++8)$ in the positive parity band $P1$. The backbending at $25/2^+$ in the band $P1$ seems to be caused by the proton pair alignment parallel to the spin of the last odd

TABLE V. Expectation values of proton and neutron numbers in the respective orbits for the yrast states of ^{89}Ru calculated with the QQ force strength A. Calculated Q moments are also tabulated.

	Proton				Neutron				
J^π	$p_{3/2}$	$f_{5/2}$	$p_{1/2}$	$g_{9/2}$	$p_{3/2}$	$f_{5/2}$	$p_{1/2}$	$g_{9/2}$	Q
$1/2^-$	3.89	5.79	0.67	5.64	3.93	5.89	1.22	5.95	−0.005
$3/2^-$	3.88	5.79	0.63	5.69	3.92	5.90	1.22	5.96	−9.1
$5/2^-$	3.88	5.79	0.64	5.69	3.94	5.88	1.22	5.96	−11.7
$7/2^-$	3.88	5.79	0.63	5.71	3.92	5.90	1.21	5.96	−17.0
$9/2^-$	3.88	5.78	0.63	5.70	3.94	5.88	1.22	5.96	−16.8
$11/2^-$	3.89	5.79	0.72	5.60	3.92	5.90	1.21	5.97	8.6
$13/2^-$	3.89	5.79	0.73	5.59	3.93	5.87	1.22	5.97	10.6
$15/2^-_2$	3.91	5.82	0.91	5.37	3.93	5.90	1.21	5.96	17.7
$17/2^-$	3.91	5.81	0.90	5.39	3.94	5.88	1.24	5.94	18.6
$19/2^-$	3.94	5.89	1.09	5.08	3.98	5.95	1.78	5.29	5.1
$21/2^-$	3.93	5.91	1.09	5.06	3.98	5.96	1.83	5.24	5.9
$23/2^-$	3.95	5.89	1.10	5.06	3.98	5.95	1.82	5.24	5.9
$25/2^-$	3.94	5.92	1.09	5.05	3.98	5.97	1.87	5.18	5.5
$27/2^-$	3.95	5.89	1.11	5.05	3.98	5.96	1.86	5.19	6.0
$29/2^-$	3.94	5.93	1.09	5.04	3.99	5.97	1.91	5.13	4.6
$31/2^-$	3.96	5.90	1.11	5.04	3.99	5.97	1.90	5.14	5.2
$33/2^-$	3.90	5.80	0.75	5.55	3.95	5.88	1.25	5.92	20.3
$35/2^-$	3.96	5.90	1.12	5.02	3.99	5.99	1.97	5.06	4.7
$37/2^-$	3.91	5.81	0.82	5.47	3.96	5.88	1.26	5.90	19.9
$39/2^-$	3.97	5.91	1.10	5.02	3.99	5.99	1.98	5.04	4.3
$41/2^-$	3.96	5.96	1.06	5.02	3.99	5.99	1.96	5.06	3.3
$7/2^+$	3.93	5.85	1.13	5.09	3.94	5.89	1.41	5.75	19.0
$9/2^+$	3.94	5.86	1.22	4.98	3.95	5.90	1.48	5.66	13.1
$11/2^+$	3.96	5.90	1.57	4.57	3.98	5.95	1.83	5.25	19.0
$13/2^+$	3.94	5.87	1.31	4.88	3.96	5.92	1.61	5.51	11.8
$15/2^+$	3.95	5.91	1.46	4.68	3.96	5.92	1.55	5.57	16.7
$17/2^+$	3.95	5.89	1.43	4.72	3.97	5.94	1.74	5.34	11.7
$19/2^+$	3.94	5.90	1.39	4.76	3.96	5.92	1.59	5.53	2.4
$21/2^+$	3.98	5.95	1.77	4.30	3.98	5.97	1.88	5.17	9.7
$23/2^+$	3.97	5.94	1.69	4.40	3.98	5.95	1.75	5.32	−5.5
$25/2^+$	3.96	5.91	1.49	4.64	3.97	5.93	1.68	5.41	3.3
$27/2^+$	3.97	5.95	1.70	4.38	3.98	5.96	1.84	5.21	−2.8
$29/2^+$	3.96	5.93	1.62	4.48	3.98	5.96	1.81	5.25	0.5
$31/2^+_2$	3.98	5.96	1.77	4.29	3.99	5.98	1.93	5.10	−3.0
$33/2^+$	3.98	5.95	1.75	4.32	3.99	5.98	1.93	5.10	−3.5
$35/2^+$	3.98	5.96	1.78	4.27	3.99	5.98	1.92	5.11	−1.7
$37/2^+$	3.98	5.96	1.78	4.28	3.99	5.98	1.93	5.10	−4.8
$39/2^+$	3.99	5.98	1.89	4.15	3.99	5.99	1.95	5.07	−5.5
$41/2^+$	3.99	5.98	1.89	4.15	3.99	5.99	1.96	5.07	−7.9

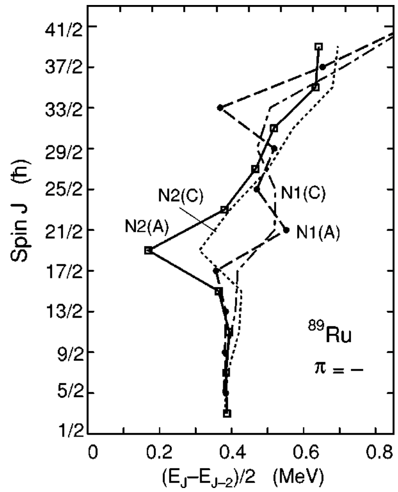

FIG. 9. The J-ω graph for the negative parity bands $N1$ and $N2$ of ^{89}Ru. The labels A and C stand for the parameter sets A and C.

neutron in $1g_{9/2}$, corresponding to the neutron pair alignment at 8^+ in ^{90}Ru. The increase of the proton number $\langle n_{g9/2}\rangle$ at $25/2^+$ testifies the proton pair alignment in $1g_{9/2}$. The small $B(E2)$ value from $25/2^+$ to $21/2^+$ and the decrease of the calculated Q moment at $25/2^+$ show the structural change there. The coincident increase of the neutron number $\langle n_{g9/2}\rangle$ at $25/2^+$ gives another evidence of strong p-n correlations in $1g_{9/2}$. For the negative parity band $N1$, the value of $B(E2:17/2^- \to 13/2^-)$ does not show any sign of such a structural change and the expectation values of proton and neutron numbers show no abrupt change, which corresponds to no backbending at 8^+ in ^{88}Ru.

Figure 9, however, predicts backbending at $33/2^-(1/2^- + 16)$ in the band $N1$. The simultaneous increases of proton and neutron numbers $\langle n_{g9/2}\rangle$ at $33/2^-$ (see Table V) say that this backbending is due to the simultaneous alignments of proton and neutron pairs ($J=16$) in $1g_{9/2}$, corresponding to the four nucleon alignment in ^{88}Ru. The small value of $B(E2:33/2^- \to 29/2^-)$ and the increase of the Q moment at $33/2^-$ testify the structure change. Figure 10 shows a sign of another backbending at $37/2^+$ in the band $P1$, which is possibly the alignment of two protons and three neutrons in $1g_{9/2}$, corresponding to the alignment at 16^+ in ^{90}Ru. The spin of the last odd neutron is parallel to the spin of rotation or alignment in the band $P1$.

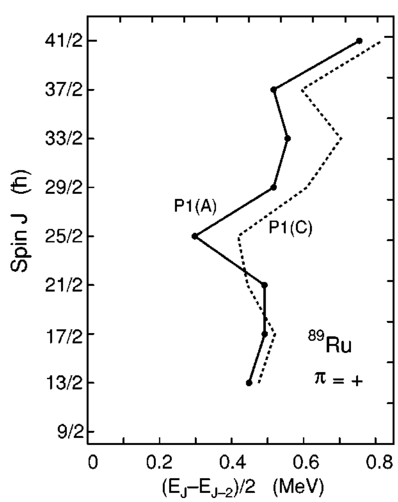

FIG. 10. The J-ω graph for the positive parity band $P1$ of ^{89}Ru.

Figure 9 shows also the J-ω graph for the negative parity band $N2$. This figure with Fig. 8 says that the low-lying collective states $3/2^-$, $7/2^-$, $11/2^-$, and $(15/2)_2^-$ of the band $N2$ and $5/2^-$, $9/2^-$, $13/2^-$, and $17/2^-$ of the band $N1$ are the partners in the angular momentum coupling $1/2^- \otimes J$ $(=J \pm 1/2)$. The similar $B(E2)$ values and similar Q moments support the picture. The most remarkable backbending in ^{89}Ru takes place at the $19/2^-$ state of the negative parity band $N2$. The small $B(E2)$ values from $19/2^-$ to $(15/2)_1^-$, $(15/2)_2^-$, and $17/2^-$ indicate a clear structure change at $19/2^-$. The Q moment decreases abruptly at $19/2^-$. For the $J \geqslant 19/2^-$ states of the band $N2$, the Q moments are nearly constant and so is the slope of J-ω graph. This phenomenon cannot be explained by the nucleon pair alignment coupled to $J=8$ $(T=1)$, because the $J=19/2$ state cannot be constructed by the coupling $1/2 \otimes 8$. If the structure change is due to a kind of alignment, the phenomenon is attributed to the p-n alignment $J=9$ $(T=0)$.

In ^{89}Ru, the efficient way to construct the $J=9$ p-n pair is one proton jump to $1g_{9/2}$. When one p-n pair aligns to $J=9$ $(T=0)$ in $1g_{9/2}$, another pair which breaks away from the α-like $2p$-$2n$ correlations is still possible to join in the monopole ($J=0,T=1$) pairing correlations, and to couple with the last odd nucleon in $2p_{1/2}$ to the total isospin $T=1/2$. The decreases of neutron and proton numbers $\langle n_{g9/2}\rangle$ at $19/2^-$ testify the decline of the α-like $2p$-$2n$ correlations due to the breaking away of the $J=9$ p-n pair from a $T=0$ $2p$-$2n$ quartet. It should be noted that the disunion of a $T=0$ $2p$-$2n$ quartet to the $T=0$ and $T=1$ pairs is prohibited for even-even nuclei. The $T=0$ p-n alignment at $19/2^-$ seems to be a unique phenomenon in the $1g_{9/2}$-subshell odd-A nuclei with $N=Z\pm 1$ such as ^{89}Ru. (The $T=0$ p-n alignment could take place in $N=Z$ odd-odd nuclei.) In this connection, the small $E2$ values from $21/2^-$ to $17/2^-$ are notable. It suggests that the p-n alignment ($J=9,T=0$) contributes to the $J \geqslant 21/2^-$ states of the band $N1$. Actually, the states $21/2^-$, $25/2^-$, and $29/2^-$ of the band $N1$ resemble the states $23/2^-$, $27/2^-$, and $31/2^-$ of the band $N2$, with respect to the energy levels, expectation values of nucleon numbers $\langle n_a\rangle$, $B(E2)$ values, and Q moments. They could be members of the collective excitations coupled with the three nucleons $2p_{1/2}^{\pi}(1g_{9/2}^{\pi}1g_{9/2}^{\nu})_{J=9,T=0}$.

The positive parity band $P2$ shows a rather complicated behavior. The very low lying $7/2^+$ state is apparently related to the state of three nucleons with $J=j-1$ in a high-spin orbit j [30]. The small $B(E2:19/2^+ \to 15/2^+)$ value and the abrupt decrease of the Q moment at $19/2^+$ testify a structure change at the $19/2^+$ state.

V. CONCLUSIONS

We have carried out the shell model calculations on the spherical basis using the extended $P+QQ$ Hamiltonian with a single set of parameters in the model space $(2p_{3/2},1f_{5/2},2p_{1/2},1g_{9/2})$. The calculations reproduce qualitatively well the overall energy levels observed in the Ru isotopes, ^{88}Ru, ^{90}Ru, ^{91}Ru, ^{92}Ru, ^{93}Ru, and ^{94}Ru. The extended $P+QQ$ model is confirmed to be useful in the heaviest $N \approx Z$ nuclei. The results testify the enhancement of the quadrupole correlations at the $N=Z$ nucleus ^{88}Ru as compared with the other Ru isotopes.

However, the disagreement between theory and experiment for ^{88}Ru cannot be disregarded. The slope of the J-ω graph showing the moment of inertia and the durable increase of angular frequency are not sufficiently reproduced for ^{88}Ru with the QQ force strength commonly fixed to all the Ru isotopes. The theoretical analysis suggests a further enhancement of the quadrupole correlations, and recommends us to use a stronger QQ force for ^{88}Ru. We have tried to strengthen the p-n QQ interaction in the two ways so as to conserve and not to conserve the isospin of eigenstates, and also to strengthen all the p-p, n-n, and p-n parts of the isoscalar QQ force. Within a small enhancement, however, there is little to choose between them in the present calculations. Anyway, the present study indicates a special enhancement of the quadrupole correlations in the $N=Z$ nucleus ^{88}Ru. This is consistent with the large deformation of ^{88}Ru in contrast to ^{90}Ru which is predicted by the projected shell model calculation on the deformed basis [4,16].

The requirement of the enhanced QQ force for ^{88}Ru possibly means that the configuration space should be extended in our spherical shell model. We have investigated the contribution of the $2d_{5/2}$ orbit which is expected to mix with the $1g_{9/2}$ orbit through the large Q matrix element. The truncated space $(2p_{1/2},1g_{9/2},2d_{5/2})$ can easily reproduce the slope of J-ω graph observed in ^{88}Ru. The result suggests that the $2d_{5/2}$ orbit contributes to the quadrupole correlations, which supports that ^{88}Ru is deformed. Contrary to this, the same calculation requires a much smaller contribution of the $2d_{5/2}$ orbit to ^{90}Ru. It is, therefore, likely that ^{88}Ru is deformed while ^{90}Ru is not largely deformed as known from the observed J-ω graphs. This situation still demands different QQ force strengths for ^{88}Ru and ^{90}Ru in our spherical shell model calculation. There is not a self-consistent way to determine the QQ force strength. An additional constraint, for instance, with respect to the Q moment value, is necessary for it. The condition is the same for the treatment on the deformed basis [4,16]. The deformation should be self-consistently determined there.

Our model with a single set of parameters, however, is capable of describing the difference between ^{88}Ru and ^{90}Ru. The calculations have presented a useful knowledge of the structure of Ru isotopes. The contrast features of ^{88}Ru and ^{90}Ru owe to the α-like $(T=0)$ $2p$-$2n$ correlations depending on the shell structure in the $1g_{9/2}$ subshell nuclei. In the ^{90}Ru isotope with one extra neutron pair which does not join in the α-like $2p$-$2n$ correlations, the extra neutron pair aligns easily to $J=9/2+7/2=8$ $(T=1)$ in $1g_{9/2}$. In contrast to this, the α-like $(T=0)$ $2p$-$2n$ correlations hinder the single nucleon-pair alignment coupled to $J=8$ $(T=1)$ till the simultaneous alignments of proton and neutron pairs at $J=2\times 8$ $(T=0)$, in the $N=Z$ even-even nucleus ^{88}Ru.

The shell structure produces characteristic bands with opposite parities in ^{89}Ru. The following predictions are obtained for ^{89}Ru. The $1/2^-$ state is the ground state. There are three characteristic bands. The negative parity band $N1$ on $1/2^-$, which resembles the ground-state band of ^{88}Ru, shows backbending at $33/2^-$ caused by the simultaneous alignments of proton and neutron pairs coupled to $J=16$ in $1g_{9/2}$. The $J\leqslant 15/2^-$ states of another negative parity band $N2$ on $3/2^-$ are the partners of the $J\leqslant 17/2^-$ states of the band $N1$. The band $N2$ shows a unique backbending at $19/2^-$ caused by the p-n pair alignment coupled to $J=9$ $(T=0)$ in $1g_{9/2}$. The positive parity band $P1$ on $9/2^+$, which resembles the ground-state band of ^{90}Ru, displays backbending due to the proton pair alignment $J=8$ $(T=1)$ parallel to the spin of the last odd neutron in $1g_{9/2}$. These predictions wait for experimental examinations.

[1] G. de Angelis *et al.*, Phys. Lett. B **415**, 217 (1997).
[2] S. M. Fischer *et al.*, Phys. Rev. Lett. **87**, 132501 (2001).
[3] N. Mărginean *et al.*, Phys. Rev. C **63**, 031303(R) (2001).
[4] N. Mărginean *et al.*, Phys. Rev. C **65**, 051303(R) (2002).
[5] A. L. Goodman, Adv. Nucl. Phys. **11**, 263 (1979).
[6] T. Marumori and K. Suzuki, Nucl. Phys. **A106**, 610 (1968).
[7] M. Danos and V. Gillet, Phys. Lett. B **34**, 24 (1971); Z. Phys. **249**, 294 (1972).
[8] A. Arima and V. Gillet, Ann. Phys. (N.Y.) **66**, 117 (1971).
[9] S. Frauendorf and J. A. Sheikh, Nucl. Phys. **A645**, 509 (1999); Phys. Rev. C **59**, 1400 (1999); Phys. Scr. **T88**, 162 (2000).
[10] K. Kaneko and J.-Y. Zhang, Phys. Rev. C **57**, 1732 (1998).
[11] K. Kaneko and M. Hasegawa, Phys. Rev. C **60**, 024301 (1999); Prog. Theor. Phys. **106**, 1179 (2001).
[12] J. A. Sheikh and R. Wyss, Phys. Rev. C **62**, 051302(R) (1999).
[13] W. Satula and R. Wyss, Phys. Lett. B **393**, 1 (1999).
[14] R. Wyss and W. Satula, Acta Phys. Pol. B **32**, 2457 (2001).
[15] Y. Sun and J. A. Sheikh, Phys. Rev. C **64**, 031302(R) (2001).
[16] Y. Sun, nucl-th/0211043.
[17] K. Hara and Y. Sun, Int. J. Mod. Phys. E **4**, 637 (1995).
[18] Y. Sun and K. Hara, Comput. Phys. Commun. **104**, 245 (1997).
[19] M. Hasegawa and K. Kaneko, Phys. Rev. C **59**, 1449 (1999).
[20] M. Hasegawa, K. Kaneko, and S. Tazaki, Nucl. Phys. **A674**, 411 (2000); **A688**, 765 (2001).
[21] K. Kaneko, M. Hasegawa, and T. Mizusaki, Phys. Rev. C **66**, 051306(R) (2002).
[22] T. Mizusaki, RIKEN Rev. **33**, 14 (2000).
[23] F. J. D. Serduke, P. D. Lawson, and D. H. Hloeckner, Nucl. Phys. **A256**, 45 (1976).
[24] H. Herndl and B. A. Brown, Nucl. Phys. **A627**, 35 (1997).
[25] M. Hasegawa and K. Kaneko, Phys. Rev. C **61**, 037306 (2000).
[26] M. Hasegawa, S. Tazaki, and R. Okamoto, Nucl. Phys. **A592**, 45 (1995).

[27] K. Hara, Y. Sun, and T. Mizusaki, Phys. Rev. Lett. **83**, 1922 (1999).

[28] G. Martinez-Pinedo, A. P. Zuker, A. Poves, and E. Caurier, Phys. Rev. C **55**, R187 (1997).

[29] A. P. Zuker, J. Retamosa, A. Poves, and E. Caurier, Phys. Rev. C **52**, R1741 (1995).

[30] A. Bohr and B. R. Mottelson, *Nuclear Structure* (Benjamin, Reading, 1975), Vol. II, p. 540.